ORIGINAL ARTICLE

# The Effect of Onset Age of Visual Deprivation on Visual Cortex Surface Area Across-Species

Adrian K. Andelin[1], Jaime F. Olavarria[1], Ione Fine[1], Erin N. Taber[2], Daniel Schwartz[2], Christopher D. Kroenke[2,3,4] and Alexander A. Stevens[2]

[1]Department of Psychology, University of Washington, Seattle, WA 98195-1525, USA, [2]Advanced Imaging Research Center, Oregon Health and Science University, Portland, OR 97239-3098, USA, [3]Division of Neuroscience, Oregon National Primate Research Center, Beaverton, OR, USA and [4]Department of Behavioral Neuroscience, Oregon Health and Science University, Portland, OR, USA

Address correspondence to Email: stevenal@ohsu.edu

## Abstract

Blindness early in life induces permanent alterations in brain anatomy, including reduced surface area of primary visual cortex (V1). Bilateral enucleation early in development causes greater reductions in primary visual cortex surface area than at later times. However, the time at which cortical surface area expansion is no longer sensitive to enucleation is not clearly established, despite being an important milestone for cortical development. Using histological and MRI techniques, we investigated how reductions in the surface area of V1 depends on the timing of blindness onset in rats, ferrets and humans. To compare data across species, we translated ages of all species to a common neuro-developmental event-time (ET) scale. Consistently, blindness during early cortical expansion induced large (~40%) reductions in V1 surface area, in rats and ferrets, while blindness occurring later had diminishing effects. Longitudinal measurements on ferrets confirmed that early enucleation disrupted cortical expansion, rather than inducing enhanced pruning. We modeled the ET associated with the conclusion of the effect of blindness on surface area at maturity ($ET_c$), relative to the normal conclusion of visual cortex surface area expansion, ($ET_{dev}$). A final analysis combining our data with extant published data confirmed that $ET_c$ occurred well before $ET_{dev}$.

Key words: blindness, cross-species, enucleation, surface area, visual cortex

## Introduction

A well-established neuroanatomical consequence of early blindness is a reduction in the surface area of the primary visual cortex (V1) of affected individuals at adulthood. This has been reported in human studies (Jiang et al. 2009; Park et al. 2009), as well as several animal species, including rats (Sugita and Otani 1984; Laing et al. 2012), mice (Massé et al. 2014), opossum (Karlen and Krubitzer 2009), ferrets (Reillo et al. 2011; Bock et al. 2012; Olavarria et al. 2012), and rhesus macaques (Rakic 1988; Rakic et al. 1991; Dehay et al. 1991, 1996). The extent of the reductions in V1 surface area varies with the timing of blindness onset (Rakic 1988; Rakic et al. 1991; Dehay et al. 1989,

1996; Karlen and Krubitzer 2009; Bock et al. 2012; Laing et al. 2013). For example, in rhesus macaques, Rakic et al. (1991), and Dehay et al. (1996) established that enucleation early in gestation produced substantial reductions in the surface area of striate cortex that were greater than when enucleation occurred at ages closer to full gestation. However, previous studies have not mapped with precision the period during which normal development of V1 surface area requires ocular input, nor determined whether this period ends at corresponding development stages across species.

The typical developmental trajectory of the surface area of V1 involves an initial expansion (Missler et al. 1993, Raznahan

et al. 2011; Knutsen et al. 2013), followed by reductions to adult size (Huttenlocher 1990; Missler et al. 1993). The effect of enucleation on the expansion of striate cortex has been linked to modulatory influences that thalamic afferents, by means of diffusible factors, exerted over early stages of corticogenesis at the level of the ventricular zone (Dehay et al. 2001; Dehay and Kennedy 2007), and to interference with the tangential migration of neurons (Reillo et al. 2011). Cortical thickness in V1 follows a similar trajectory as surface area: initial expansion, overshooting and then reduction to adult levels (Huttenlocher 1990; Missler et al. 1993). Blindness also results in increased V1 cortical thickness, which has been interpreted in human studies as resulting from reduced synaptic pruning later in development (Bridge et al. 2009; Jiang et al. 2009; Anurova et al. 2015). Our primary goal was to determine if there is consistency in the timing of the effects of blindness on V1 surface area expansion in rats, ferrets and humans, and investigate if early enucleation reduces surface area size by interfering primarily with cortical expansion. We report that the effect of blindness on V1 surface area ends before surface area expansion is complete, and prior to peak synaptic density in V1.

Human studies of blindness have relied on anatomical MRI to measure alterations in visual cortex as a consequence of blindness (Ptito et al. 2008; Bridge et al. 2009; Jiang et al. 2009; Park et al. 2009; Leporé et al. 2010; Anurova et al. 2015). In humans, age of onset of blindness can usually only be estimated from the etiology of blindness (e.g., anophthalmia, retinopathy of prematurity (ROP), injury to the eyes, etc.). Furthermore, human studies of blindness are almost uniquely conducted at adulthood, and consequently, the reduction in surface cortical area may reflect the effects of blindness on the expansion in surface area that occurs early in development, or as a result of synaptic and axon elimination, which occurs later in development (Huttenlocher 1990; Missler et al. 1993; Bourgeois and Rakic 1993). Knowing when the effect of blindness no longer influences the surface area of visual cortex would be useful to further our understanding of the mechanisms controlling cortical growth, and to guide the interpretation of the effects of blindness onset on human cortical surface area development.

To bridge the findings between animal and human studies, we examined how the age of blindness onset affects surface area of V1 at adulthood in rats, ferrets, and humans. To facilitate inter-species comparisons, blindness onset was expressed in terms of a species-independent timeline of neuro-developmental event times (ET) (Finlay and Darlington 1995; Darlington et al. 1999; Clancy et al. 2007; Workman et al. 2013). Animal models consisted of rats and ferrets bilaterally enucleated (BE) at defined postnatal ages, and sighted control (SC) animals. Human subjects included anophthalmic (in which both eyes fail to develop), congenitally-blind (in which pattern vision never develops), late-onset blind (following development of relatively normal pattern perception), and normally-SC. We used histological methods in rats, a longitudinal structural MRI study in ferrets, and structural MRI data from ferrets and humans to identify a common developmental endpoint for the effect of blindness on primary visual cortex surface area. Our results provide evidence that blindness disrupts cortical expansion, and that the critical period for the effect of enucleation on visual cortex surface area ends before V1 surface area reaches its normal adult size. These data suggest that visual cortex expansion remains susceptible to visual deprivation through the perinatal period, followed by a later stage during which expansion is largely independent of ongoing visual input.

## Materials and Methods

### Animal Care

All procedures were approved by the relevant Institutional Animal Care and Use Committee, and were carried out in accordance with the NIH Guide for the Care and Use of Laboratory Animals.

### Rats

#### Animal Numbers
A total of 56 rats were included in these experiments. A set of 40 were BE at eight postnatal ages. The day of bilateral enucleation (BEP) is indicated with the postnatal day in which enucleation was performed: within 24 h of birth (BEP0; $n = 6$), BEP10 ($n = 4$), BEP12 ($n = 5$), BEP14 ($n = 6$), BEP16 ($n = 5$), BEP25 ($n = 5$), BEP30 ($n = 5$), BEP45 ($n = 4$). Six sighted rats served as controls (SC). All measurements were made at maturity (>P60). The remaining ten rats were used to study the development of the surface area of V1 in normally sighted animals, sacrificed at P30 ($n = 5$) and P35 ($n = 5$) (Table 1).

#### Experimental Procedures
Pregnant animals were monitored several times daily and the births of the litters were determined to within 12 h (the first 24 h correspond to P0). Rats were injected with ketofen (0.05 mg/kg, i.p.) and anesthetized with isoflurane (2–4% in air). After full recovery from surgery, rat pups were either returned to their dams, or to their home cage if the enucleation took place after weaning. Enucleated rats received daily i.p. injections of ketofen for three additional days. Upon reaching maturity, experimental as well as control rats were deeply anesthetized with pentobarbital sodium (100 mg/kg i.p.) and perfused transcardially with 0.9% saline followed by 4% paraformaldehyde (PFA) in 0.1 M phosphate buffer (PB, pH 7.4). A

**Table 1** Rat enucleated groups and sighted controls.

| Group | Enucleation age | Sample size | Event time | V1 Surface area | Cortex surface area | Ratio V1:Cortex | % Adult VSAR |
|---|---|---|---|---|---|---|---|
| BEP0 | P0 | 6 | 0.43 | 9.3 | 166.9 | 0.06 | 73.3 |
| BEP10 | P10 | 4 | 0.66 | 12.0 | 181.3 | 0.07 | 86.8 |
| BEP12 | P12 | 5 | 0.70 | 12.5 | 181.7 | 0.07 | 90.0 |
| BEP14 | P14 | 6 | 0.73 | 13.2 | 185.2 | 0.07 | 93.3 |
| BEP16 | P16 | 5 | 0.76 | 13.0 | 179.1 | 0.07 | 94.8 |
| BEP25 | P25 | 5 | 0.89 | 13.3 | 182.4 | 0.07 | 95.7 |
| BEP30 | P30 | 5 | 0.95 | 13.7 | 186.5 | 0.07 | 96.5 |
| BEP45 | P45 | 4 | 1.10 | 13.9 | 185.8 | 0.07 | 98.2 |
| SC | >P60 | 6 | 1.30 | 14.3 | 185.5 | 0.08 | 100.0 |

similar procedure was used to anesthetize and perfuse the animals used to study the development of the area size of V1.

A histological approach was used to measure visual cortex surface area. The surface areas of primary visual cortex and remaining isocortex were measured using tangential sections from physically-flattened cortical mantles. Brains were removed from the skull and the entire cortical mantle was separated from the brain stem, flattened between glass slides and left in 0.1 M PB for 24 h. The tissue was then transferred to 4% PFA in 0.1 M PB, 20% sucrose solution for an additional hour and cut tangentially to the cortical surface (60-μm sections collected in 0.1 M PB). Unstained tangential sections were scanned at 2400 dpi (Epson 4990) to identify the border of V1 based on the myelin pattern (Fig. 1a, b). The myelin pattern was optimally displayed in tangential sections passing through Layer 4 (500–650 μm deep), and the sharp transition from dense to
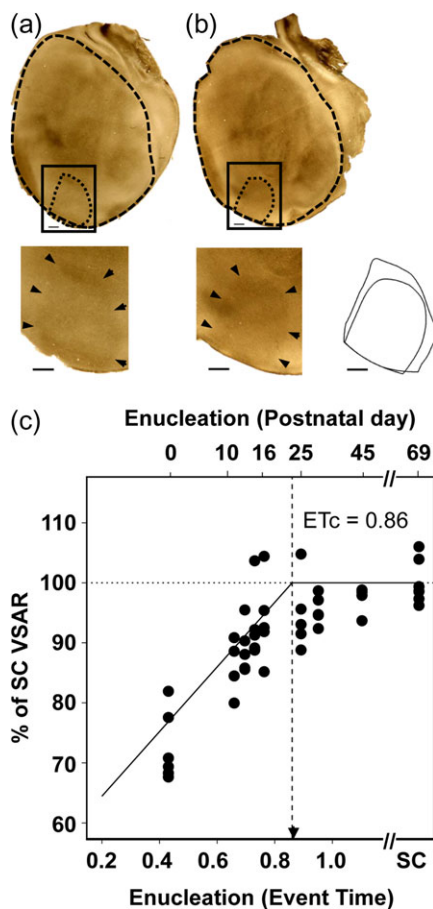


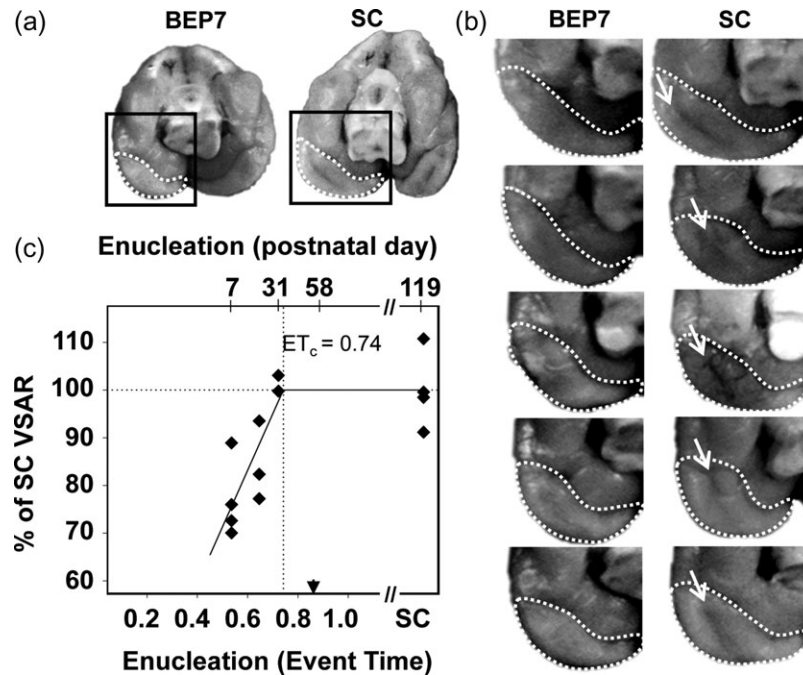**Figure 1.** Rat primary visual cortex surface area as a function of age of deprivation onset in bilaterally enucleated rats. Profiles of V1 and cortical mantle revealed in tangential sections for **(a)** SC rat measured at postnatal day (P) 60 rat and **(b)** a BEP12 rat. In both visual cortices, heavily-stained myelinated regions allow delineation of primary visual cortex (dashed black line). Inset shows the overlaid outlines of V1 surfaces of the P60 control and BEP12 rat, illustrating the reduced surface area of the BEP12 hemisphere compared with control. Scale bars = 1 mm. **(c)** Percent of adult sighted control VSAR, for rats enucleated over an age range extending from P0 (ET = 0.43) to P45 (ET > 1). A second abscissa indicates the postnatal day at which binocular enucleation was performed. The solid line indicates the piece-wise regression line of best fit (adjusted $R^2$ = 0.69). Vertical dotted line indicates the estimated end of the effect of enucleation ($ET_c$ = 0.86). Arrowhead indicates V1 peak synaptic density. SC = sighted control, VSAR = Primary visual to non-visual cortex surface area ratio.

reduced myelination at the border of V1 was delineated in two or more sections from the same animal with the aid of the filter "trace contour" in Adobe Photoshop CS5 (Adobe Systems, CA). This method has been applied in previous work (Richter and Warner 1974; Laing et al. 2012; 2013; 2015) as an effective method for delineating borders of V1 in tangential sections. The borders of the cortical mantle and V1 were reconstructed by carefully aligning sections using the edges of the sections, sulci, blood vessels, and other fiducial marks. Data from animals, BE at P0 through P45 were compared with corresponding data from 60-day-old SC animals. Once borders of V1 had been defined using the trace contour filter in Photoshop, measurements of each area were taken in pixel count and then converted to surface area.

## Ferrets

### Animal Numbers

A total of 25 ferrets were examined using live and postmortem MRI. Ferret litters were purchased from Marshall Bioresources (North Rose, NY) and delivered to Oregon Health and Science University ($N$ = 23 animals) or Washington University ($N$ = 2 animals) on postnatal Day 5 (gestation in ferrets = 41 days), where subsequent procedures were carried out. Thirteen ferrets were included in the comparison of the effect of enucleation at different ages on V1 surface area (Table 2). Of these, nine [BEP7 ($n$ = 3), BEP20 ($n$ = 3), SC ($n$ = 3)] were part of a previous study (Bock et al. 2012), and an additional four ferrets [BEP7 ($n$ = 1), BEP31 ($n$ = 2), SC ($n$ = 1)] were also included. All were euthanized at adulthood (P120 or older), and their brains were perfused with 4% PFA. Two additional groups of ferrets, BEP7 ($n$ = 3) and SC ($n$ = 3), underwent postmortem MRI at P31, and an additional two groups BEP7 ($n$ = 3) and SC ($n$ = 3), underwent longitudinal MRI experiments. All 12 animals were perfused on Day P31 with 4% PFA following previously described procedures (Bock et al. 2012).

### Experimental Procedures

Ferrets examined by postmortem MRI were euthanized and perfused with 4% PFA. The extracted brains were imaged following previously described procedures for brains analyzed at adulthood (Bock et al. 2012) or at P31 (Bock et al. 2010). In a follow-up longitudinal experiment, BEP7 and SC ferrets were examined using *in vivo* MRI over the postnatal period from P11 to P28. For both the BEP7 and SC groups, two animals were scanned at P14, P21, and P28, while the third ferret was scanned at P11, P18, and P25, using experimental procedures (and data from two SC animals) described previously (Knutsen et al. 2013). The brains were scanned using an 11.7 T static magnetic field strength magnet interfaced with a small animal imaging gradient system capable of producing highly similar maximum gradient strengths (of 70 G/cm), as well as an identical volume coil transmit/surface coil receive radiofrequency coil configuration.

Following image acquisition and cerebral cortex reconstruction (Bock et al. 2010; Knutsen et al. 2013), gyral/sulcal landmark-based conventions reported previously were used to define boundaries of the isocortex and V1 (see Bock et al. 2012, and references therein). Briefly, on the ventral lateral surface of the brain, the border of the isocortex corresponds to the fundus of the rhinal fissure, and to the dorsal edge of the corpus callosum on the medial surface of the brain. Primary visual cortex was defined as the area (outlined in red in Figs 2, 5) extending from the fundus of the splenial sulcus to the occipital crest, and from the dorsal-most point on the medial cortex to the

**Table 2** Ferret enucleated groups and sighted controls measures.

| Group | Enucleation age | Sample size | Event time | V1 Surface area | IsoCortex surface area | Ratio V1:Ctx | % Adult VSAR |
|---|---|---|---|---|---|---|---|
| BEP7 | PC48 | 4 | 0.54 | 55 | 781 | 0.076 | 78.1 |
| BEP20 | PC61 | 3 | 0.65 | 65 | 852 | 0.082 | 85.1 |
| BEP31 | PC72 | 2 | 0.72 | 70 | 774 | 0.099 | 102.5 |
| SC | >119 | 4 | >1 | 67 | 759 | 0.096 | 100.0 |



Figure 2. Primary visual cortex surface area as a function of age of deprivation onset in bilaterally-enucleated ferrets. (a) The primary visual cortex resides on the medial occipital surface, indicated by dashed white boundaries in caudal/ventral views of the brain in a BEP7 and a sighted control (SC) ferret. Although the primary visual cortex in ferrets extends dorsally, the surface area reduction in brains of BEP7 ferrets is notable in the ventral cortex due to the absence of the occipital-temporal sulcus. (b) The surface area of the primary visual cortex (enclosed by dashed boundaries) of BEP7 ferrets is reduced compared with controls. The absence of the occipital-temporal sulcus in BEP7 animals (arrows in control brains), contributes to the difference in visual cortex surface area. (c) Quantification of VSAR by MRI revealed pronounced reductions in early enucleates (P7, ET = 0.54), with graded effects of enucleation on the primary visual to non-visual surface area ratio for later enucleations (P20, ET = 0.65 and P31, ET = 0.72). The Solid line indicates best fit of the piece-wise regression (Adjusted $R^2$ = 0.64). Vertical dotted line indicates the estimated end of the effect of enucleation (ETc = 0.74). Arrowhead indicates V1 peak synaptic density. Abbreviations as in Fig. 1.

ventral extreme of the occipital-temporal sulcus (yellow arrows, Fig. 2b). This region corresponds to an area that is largely devoid of inter-hemispheric connections and was identified as ferret primary visual cortex by Bock et al. (2012).

## Humans

### Subjects

Data from 51 human subjects were included in the study. The data included five participants with anophthalmia (AN), 14 with early-onset blindness (EB), 9 with late-onset blindness (LB), and 23 SC, collected at three laboratories (Supplementary Table S1). Acquisition procedures were described previously (Stevens et al. 2007; Bridge et al. 2009; Bock et al. 2015; Jiang et al. 2016). Six AN and nine SC participants were scanned on a 7 T Siemens/Magnex system at Oxford University (Bridge et al. 2009). Nine EB, 5 LB, and 10 SC subjects were scanned in a Siemens 3 T Trio with a 12-channel head coil, at Oregon Health and Science University (Stevens et al. 2007). Five EB participants and four SC participants were scanned in a Siemens 3 T Trio with a 12-channel head coil, at Oxford University (Bridge et al.

2009). A group of 4 LB participants were scanned in a Philips Achieva 3 T with a 32 channel head coil. The severe atrophy of optic nerves in these AN individuals was previously confirmed with T1-weighted MR scans (Bridge et al. 2009). (Descriptions of individuals in the AN, EB, and LB are provided in Supplementary Table S1). All participants provided written informed consent in accordance with the Institutional Review Board of each respective site.

### Experimental Procedures

In humans, consistently detecting the stria of Gennari with MRI is challenging, and its presence is debated in Anophthalmic individuals (Trampel et al. 2011). However, retinotopic mapping of visual cortex with fMRI has demonstrated that cortical topology in and around the calcarine sulcus is closely coupled to the orientation and extent of visual fields (Hinds et al. 2008; Benson et al. 2012), and striate cortex can be estimated with high precision from the cortical folding patterns along the calcarine sulcus in blind individuals (Jiang et al. 2009; Park et al. 2009). All MRI 3D datasets were processed for landmark-based segmentation and surface reconstruction using the Freesurfer software
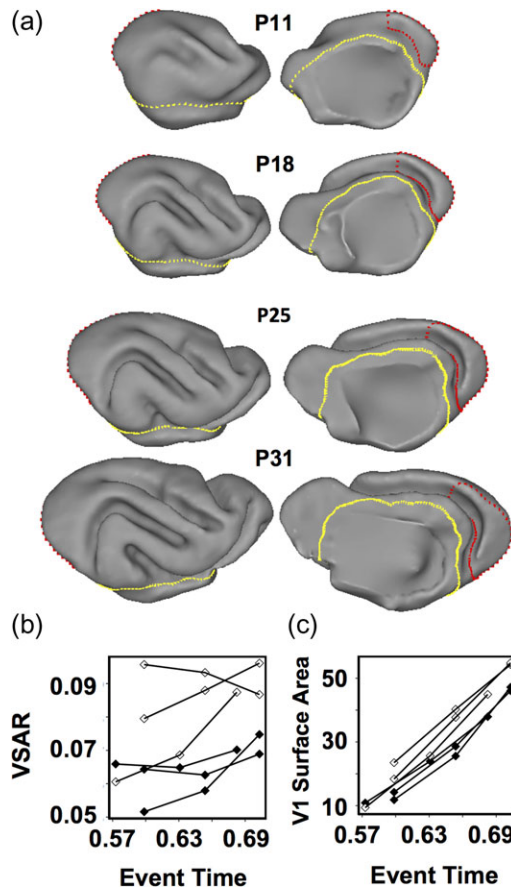
**Figure 5.** Longitudinal MRI anatomical analysis in three sighted control ferrets and three ferrets enucleated at P7. The visual cortical surface area is reduced in the immature brain of P7 enucleated ferrets, compared with that in immature brains of control ferrets. **(a)** Lateral (left) and medial (right) views of the right hemisphere of a control ferret brain at ages P11, P18, P25, and P31. Gyri and sulci appear as they do in a mature brain, which enables delineation of striate visual cortex (red), as well as isocortex (yellow) boundaries following previously established conventions (Bock et al. 2012). **(b)** VSAR plots of the average of the left and right primary visual cortex surface area for three control (open symbols) and three BEP7 (black symbols) ferrets illustrating the reduction in surface area in the BEP7 ferrets induced by the enucleation. **(c)** Plots for the same animals, as in b, but showing V1 surface area (mm²) expansion over time.

toolkit (http://freesurfer.net/) using the "recon-all" function with default settings. A full description of the processing steps is online: (https://surfer.nmr.mgh.harvard.edu/fswiki/recon-all). Briefly, each brain dataset is intensity normalized, affine transformed to a Talairach atlas space, and skull-stripped. The boundary between white matter and gray matter is determined throughout the brain using intensity, neighborhood and smoothness constraints. The space between the pial surface and white matter boundary is then tessellated, and smoothed to create a cortical ribbon. The cortical ribbon is then parcellated and neuroanatomical labels of brain areas are assigned to each voxel based on probabilistic anatomic information and gyral and sulcal landmarks (Dale et al. 1999; Fischl et al. 2002; Fischl 2004). The primary visual cortex has been demonstrated through cytoarchitectural analyses to be reliably identified by gyral and sulcal folds (Fischl et al. 2008). The reconstructed cerebral cortex surface and boundaries for primary visual cortex for each subject were reviewed by three study staff, blind to the group assignment of the brain.

## Calculation of Primary Visual to Non-visual Cortex Surface Area Ratio and Between-Species Comparisons

The surface area of V1 varies with the whole cortical surface of the brain. Therefore, to control for the effect of inter-individual variability in brain size on the V1 surface area, the V1 surface area was quantified as a ratio of V1 surface area and the surface area of the remaining cortical mantle (i.e., isocortex surface area minus the V1 surface area). The V1 surface area ratio (VSAR) from each experimental group can also be used to compare with the VSAR of sighted adults of the same species, providing an unbiased measure of the percentage of reduction in surface area as consequence of age at blindness onset. Specifically, to directly compare the effect of age at blindness onset on surface area reduction of V1 across species, the VSAR of each experimental group was expressed as the percentage of the corresponding SC group (% VSAR = $100 * VSAR_{blind} / VSAR_{SC}$).

All data are expressed in a common developmental timeframe, using the "translating time" regression model developed by Finlay and colleagues (Workman et al. 2013; see also, http://www.translatingtime.org). This model provides a regression equation that translates early neuro-developmental events into species-independent ET that spans early brain development, allowing for the prediction of 271 developmental events across 18 mammalian species. The parameters of ET and post-conception (PC) age (in days) are related through the expression

$$ET = (ln(PC) - Constant)/Slope$$

Species-specific *Constant* and *Slope* parameters are given in Table 2 of Workman et al. (2013) and on the translating time website (www.translatingtime.org). PC at birth for rats = 21 days, ferrets = 41 days, and humans = 270 days.

## Statistical Analyses

The effects of visual deprivation on V1 surface area measured at adulthood can be characterized by a linear function that reflects the relationship between age at blindness onset and the resulting reduction of V1 surface area at adulthood. We define the event time, $ET_c$, such that blindness occurring after $ET_c$ no longer affects V1 surface area expansion. After $ET_c$, V1 surface area should achieve the V1 surface area of adult SC conspecifics, reflecting no further effect of blindness on V1 surface area. We estimated $ET_c$ for each species using a non-linear piece-wise regression model. The model uses a two-segment fitting algorithm: a linear estimate of the best fitting line to the data with values less than 100% of adult VSAR and a flat line reflecting the values that do not differ from the mean of the adult VSAR value. (i.e., the ET at which VSAR reaches 100% of the adult VSAR). The piece-wise model is expressed as follows:

Percent of Adult VSAR = $[(m*x + b|x < ET_c), (100\%|x > ET_c)]$

where (*b*) is the y-intercept, (*m*) is the linear regression slope, (*x*) is age of blindness onset (expressed in ET), and ($ET_c$) is the ET at which VSAR reaches 100%. $ET_c$ denotes the event time at which blindness onset no longer reduces V1 surface area (i.e., the measurement of VSAR is 100% of the adult control VSAR). All analyses were carried out with R (https://www.r-project.org/) using the *nls* function, and an iterative minimization of least squares approach to find the value of $ET_c$.

## Results

### The Effect of Age of Visual Deprivation Onset on Adult Primary Visual Cortex Surface Area

#### Rats

Figure 1 shows the flattened-primary visual cortex of a SC rat at P60 (Fig. 1a), and of a BEP12 rat (Fig. 1b), also sacrificed at P60, illustrating the reduction in surface area as a consequence of enucleation at P12. Figure 1c plots the percent of adult VSAR as a function of the ET at which enucleation was performed. The area size of V1 in rats BE on P0 (BEP0, ET = 0.43) through P45 (BEP45, ET > 1) are plotted as the percent of the mean adult SC VSAR (all animals were sacrificed at P60). In adult SC rats, ~8% of the cortical surface area is occupied by V1. In contrast, for rats enucleated at P0 the surface area of V1 measured at maturity is reduced to roughly 6% of the cortical surface area, in agreement with previous studies (Laing et al. 2012).

Early enucleation (e.g., BEP0, ET = 0.43) produced much larger reductions in VSAR than later enucleations, with a strong linear relationship between age of enucleation and percent adult VSAR, over the measured age range (Fig 1c). Enucleation age had a strong linear relationship to percent of adult VSAR (adjusted $R^2$ = 0.69) (Fig 1c). The estimated age when an effect of enucleation on VSAR has concluded, $ET_c$ = 0.86, corresponds to a postnatal age of 22.6 days in rats.

#### Ferrets

In this species, most of primary visual cortex resides on the caudal and medial part of the brain, and its borders can be readily identified by sulcal landmarks (Fig. 2a) (see Materials and Methods, and Bock et al. 2012). Figure 2b shows boundaries used to estimate the V1 surface area in five animals enucleated at BEP7 and in five SC animals. The ventral view shown in Fig. 2b highlights the fact that early enucleation reduces cortical folding within primary visual cortex: the occipital-temporal sulcus, observed in adult SC animals (yellow arrows in Fig. 2b) is not observed in adult ferrets enucleated at P7 (ET = 0.54). The effect of enucleation on the area size of V1 was analyzed at adulthood in ferrets enucleated at P7 (ET = 0.54), P20 (ET = 0.65), and P31 (ET = 0.72) (Table 2). Relative to the size of area V1 in SC ferrets, we observed that the surface area of V1 is reduced in enucleated ferrets, with a graded effect of age of deprivation similar to that observed in rats (Fig. 2c). The piece-wise regression demonstrated a strong linear association between age of enucleation and percent of adult SC VSAR (adjusted $R^2$ = 0.64), indicating that enucleation ceases to affect the surface area of V1 at $ET_c$ = 0.74, corresponding to postnatal age of 39 days. Table 3 lists the regression model parameters and fits of the piece-wise regression models for enucleated and SC rats and ferrets.

**Table 3** Piece-wise regression parameter estimates of percent adult VSAR by time of enucleation for Enucleated Rats, Sighted Rats (normal development of V1 size), Enucleated Ferrets, data combined across species for blind and sighted animals.

| Group | Parameter estimate | Standard error | T-value |
|---|---|---|---|
| Rat: Enucleated | | | |
| y-intercept | 52.17 | 3.57 | 17.46*** |
| Slope | 54.66 | 4.81 | 8.04*** |
| $ET_c$ | 0.86 | 0.05 | 18.47*** |
| Adjusted $R^2$ | 0.69 | | |
| Rat: Sighted | | | |
| y-intercept | −26.37 | 13.27 | −1.92 |
| Slope | 119.64 | 15.36 | 7.79*** |
| $ET_{dev}$ | 1.056 | 0.04 | 27.08*** |
| Adjusted $R^2$ | 0.76 | | |
| Ferret: Enucleated | | | |
| y-intercept | 12.16 | 21.94 | 0.55 |
| Slope | 118.34 | 33. 46 | 3.34* |
| $ET_c$ | 0.742 | 0.056 | 11.12*** |
| Adjusted $R^2$ | 0.64 | | |
| All Species: Blind | | | |
| y-intercept | 23.87 | 8.72 | 2.73** |
| Slope | 95.28 | 16.08 | 5.92*** |
| $ET_c$ | 0.75 | 0.08 | 9.38*** |
| Adjusted $R^2$ | 0.53 | | |
| All Species: Sighted | | | |
| y-intercept | −50.75 | 19.75 | −2.56 |
| Slope | 152.75 | 26.08 | 5.86*** |
| $ET_c$ | 0.91 | 0.39 | 22.92*** |
| Adjusted $R^2$ | 0.57 | | |

* 0.01, ** 0.001, *** < 0.001.

#### Humans

Human data came from of three groups of subjects blinded at different ages. In one group, blindness was due to anophthalmia (AN), in which the midbrain, diencephalon and cortex never receive retinal input because retinal projections fail to develop. We confirmed the severe atrophy of optic nerves in the AN individuals with T1-weighted MR scans (Bridge et al. 2009). The early blind group (EB) consisted primarily of individuals with ROP. Unlike AN subjects, the midbrain, diencephalon and cortex of EB subjects receive retinal input before the onset of blindness, which occurs neonatally. The late blind (LB) group consisted of individuals who, after relatively normal visual development, lost their vision due to disease or accidents affecting the eyes at 7 years of age or later (Table 4). Data from one EB subject were discarded after noting the highly abnormal cerebral cortical surface generated by Freesurfer, which upon visual inspection of the input images, revealed artifacts consistent with substantial motion during the MPRAGE scans.

Primary visual cortex and the whole cortical surface of a representative SC are shown in Fig. 3a. As in rats and ferrets, the reduction of the VSAR in humans depends on the age of blindness onset (Fig. 3b). To characterize the differences between the groups of blind individuals, we determined if the age of blindness onset produced a monotonic increase in VSAR. Based on our rat and ferret data, we predicted that both AN and EB groups would have smaller VSAR than the SC group, but the LB group, due to blindness onset after surface area expansion was complete, would have similar VSAR values to the SC group. However, because the precise age of onset could not be determined for AN and EB subjects, we analyzed the human data

**Table 4** Human surface area means by hemisphere.

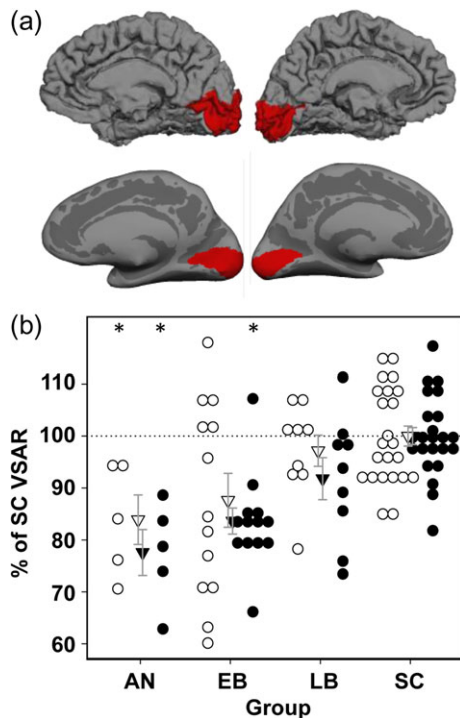| Group | N | Event time | V1 Surface area[a] Left | Right | Cortex surface area[a] Left | Right | % SC VSAR Left | Right |
|---|---|---|---|---|---|---|---|---|
| AN | 5 | 0.32 | 2027 | 2109 | 90 447 | 89 298 | 83.90 | 77.58 |
| EB | 14 | 0.65 | 1823 | 1993 | 78 703 | 78 982 | 87.62 | 83.63 |
| LB | 9 | >1.0 | 2006 | 2196 | 77 726 | 79 657 | 97.18 | 91.80 |
| SC | 23 | – | 2285 | 2612 | 86 793 | 86 878 | 100.00 | 100.00 |

[a]Areas in mm$^2$.

Figure 3. Primary visual cortex surface area reduction in humans, associated with anophthalmia (AN), early-onset blindness (EB) late-onset blindness (LB) and sighted controls (SC) (see Methods, for group details). (a) For a SC subject, the region of cerebral cortex assigned to V1 is indicated by red areas. A fiducial surface of each cerebral hemisphere is shown in the top row and the corresponding inflated surface is shown in the bottom row. (b) VSAR for AN, EB and LB groups expressed as a percentage of SC VSAR for left (open circles) and right (closed circles) hemispheres. Significant VSAR reductions are observed in both left and right hemispheres for AN, and in the right hemisphere EB, relative to SC (*P < 0.05, corrected for multiple comparisons).

using non-parametric estimates of group differences, comparing each of the blind groups to the SC group. The analysis was performed with the *nparcomp* package (Konietschke et al. 2015) implemented in R (https://www.r-project.org/). The significance level was maintained at $P < 0.05$ across group comparisons. In the AN group bilaterally, the VSAR was significantly smaller than in the SC group. In the EB group, VSAR was significantly smaller in the right hemisphere, but the reduction in VSAR did not reach significance in the left hemisphere of the EB group compared with the SC group. As predicted, the LB group did not differ significantly from the SC group (Fig. 3b). We also compared the groups' isocortex surface area and found that the AN, EB, and LB did not differ significantly from the SC group, although there was a trend toward a smaller surface area in the EB group relative to the SC group (see Table 4).

A subset of EB participants had some residual light sensitivity or had a history of minimal light perception prior to onset of complete blindness. To determine if minimal diffuse light sensitivity influenced surface area, we compared VSAR measurements between EB individuals with residual light perception ($n = 4$, mean = 0.023 ± 0.004), to those without residual light perception ($n = 9$, mean = 0.026 ± 0.004). For both subgroups of EB subjects, the VSAR is approximately equal to the mean VSAR for EB subjects overall (Table 4). There was a trend for those EB with light perception to have a slightly larger VSAR than those EB without light perception (Wilcoxon rank sum test: $Z = 1.778$, $P = 0.08$). Therefore, we cannot completely rule

out the effect of mere light exposure on V1 surface area in the EB subjects.

### Rat–Ferret–Human Comparisons

Figure 4 combines our data on the effects of age of blindness onset on the area size of V1 from rats (circles), ferrets (diamonds) and humans (inverted triangles). Each pointed is weighted by the square-root of the sample size of the contributing observations. Unlike the experimental animal data, in which the age at enucleation is known precisely, human blindness onset is rarely known precisely for AN and EB individuals (Verma and Fitzpatrick 2007). For AN humans, we used PC78 (ET = 0.32) as the approximate time of blindness onset, which corresponds to the ET in which optic axons reach the dorsal lateral geniculate nucleus in normal visual development. Severe ROP, as was the case in our EB subject group, is detectable 4 weeks prior to the normal 40 week (PC = 270 days) gestation period for humans, corresponding to a blindness onset age of PC242 (ET = 0.62). In the LB group blindness occurred over a broad age range well above the range of the ET scale; therefore, these data were excluded from the graph. All but 2 LB subjects were post-adolescent, and in the remaining two subjects, blindness occurred at ages 7 and 12, so it can be presumed that cortical expansion was virtually complete. As shown in Fig. 4, the model fit was good (adjusted $R^2 = 0.62$), and the cross-species $ET_c = 0.82$, in good agreement with the $ET_c$ estimated for rats and ferrets separately.

### Early Blindness Attenuates Visual Cortex Expansion

The finding that the critical period for the effect of blindness ends relatively early in the developmental timeline suggests that the effect of visual deprivation on surface area might result from attenuated expansion of visual cortex, rather than by increasing the synaptic pruning that typically occurs at later stages of development. However, because the effect of delayed blindness onset was assessed at adulthood, after both expansion and pruning have taken place, it remains possible that both processes contribute to reduced surface area at maturity. To more directly examine whether early enucleation reduces cortical expansion, we carried out longitudinal MRI measurements of VSAR during the expansion phase of cortical
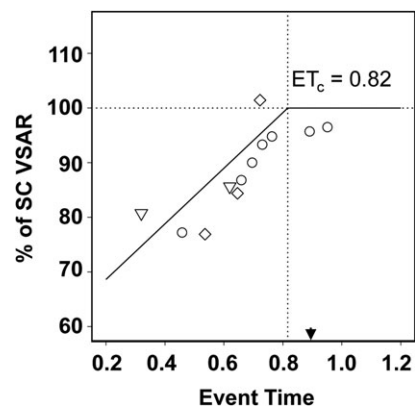


Figure 4. Effect of age of blindness onset on the area size of V1. Data from blind rat, ferret, and human groups reported in the current study fit with a piecewise regression model. The piece-wise regression model of best fit yields the estimate of $ET_c = 0.816$ (vertical dotted line) as the event time at which blindness no longer affects the size of V1 surface area (adjusted $R^2 = 0.62$). Arrowhead indicates V1 peak synaptic density.

maturation, from P11 (ET = 0.57) through P28 (ET = 0.70), in three ferrets enucleated at P7 (ET = 0.54) and three SC ferrets.

Figure 5a illustrates that by age P11, gyral and sulcal folds, although rudimentary, provide sufficient information to delineate striate (red borders) and isocortical (yellow borders) boundaries using the methods applied to adult brains (see Materials and Methods, and Bock et al. 2012). By P25, these landmarks are highly similar to the pattern observed in adult brains. Figure 5c shows that, over the period from P11 through P28, striate cortex in the control animals (open symbols) expands linearly at a rate of 2.5 mm$^2$/day. Differences between BEP7 (closed symbols) and SC animals are apparent by P14 (ET = 0.6), 1 week following enucleation. Figure 5b illustrates that VSAR of the immature cortex is significantly reduced in BEP7 animals compared with controls ($Z(4) = 1.964$, $P = 0.05$). Similar findings occurred in a cross-sectional analysis performed on postmortem tissue for separate groups of three BEP7 ferrets (VSAR = 0.816) and three SC ferrets (VSAR = 0.944) at P31, again, indicating significantly reduced VSAR in the BEP7 animals compared with SC ferrets ($P = 0.009$; data not shown). Notably, VSAR in the BEP7 animals measured prior to P31 was 77% of the VSAR in SC animals in the longitudinal measurements, and 85% for animals assessed at P31 in the postmortem analysis, which corresponds well with the 75% of SC VSAR observed in mature ferrets enucleated at P7 (Fig. 2). Thus, the effects of early enucleation are similar in magnitude regardless of whether measurements are made at P14 (ET = 0.6), or in the adult animal. This strongly suggests that perturbed cortical expansion, rather than enhanced pruning, is the primary mechanism underlying reduced V1 surface area in visually deprived animals.

### Blindness Ceases to Affect the Surface Area of V1 Well Before Expansion of V1 is Complete

Is expansion of visual cortex susceptible to the effects of blindness until V1 reaches its normal adult size? Answering this question is important for understanding the role of visual input in the maturation of visual cortex. In the rat, Duffy et al. (1998) reported that V1 surface area expansion continues beyond P27, past the age at which our data indicate that enucleation no longer affects the size of area V1 (P22.6, $ET_c = 0.86$) (Fig. 1c). To determine the end of the growth period, we measured the size of V1 at P30 ($n = 5$), P35 ($n = 5$), and P60 ($n = 6$) in control rats and plotted these data, and that from Duffy et al. (1998), in Fig. 6 (blue symbols). Application of the same regression model to these developmental rat data lead to the estimation that the event time corresponding to the conclusion of surface area expansion, $ET_{dev}$ is 1.05. This result, together with our data from the BE rats, indicates that blindness starting by ET = 0.86 no longer has a significant effect on the expansion of V1 even though V1 is still significantly smaller (by about 25%) than its adult size. Table 3 lists the regression model parameters and significance of the piece-wise regression models used for the rat developmental data.

### Analysis of Published Data in Other Species

In studies that provided a surface area measures of the isocortex as well as V1, we calculated VSAR as described above. For studies in which isocortical surface area was not provided, we calculated the ratio of surface area of V1 of the blind sample to the average V1 surface area of adult sighted conspecifics. Although this approach does not provide a bias correction for
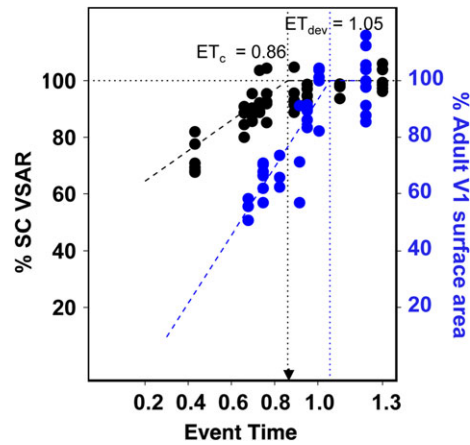


**Figure 6.** Comparison of the effect of age of blindness onset on the area size of V1 with the normal development of V1 in sighted rats. Data from the enucleated rats in Fig. 1c (black circles) are plotted with data from normally developing rats (blue circles) sacrificed at ages P11, P15, P20, and P27 replotted from Duffy et al. (1998), and P30 and P35 collected in the present study. Because Duffy et al. (1998) did not report measurements for the non-visual isocortex, the surface area values for V1 were normalized by dividing them by the size of V1 measured in the respective adult sighted control rats and the ratio was expressed as % of adult size of V1 (blue Y-axis legend). Exact ages of the adult rats in Duffy et al. (1998) were not specified, but were set at P69 (ET > 1.2). $ET_{dev}$ is the estimated ET at which V1 surface area reaches adult size.

individual differences in total cortical surface area, evidence suggests that enucleation does not induce changes in total cortical surface area (e.g., Rauschecker et al. 1992; Bock et al. 2012; Laing et al. 2012). Our analysis included histological studies in rhesus macaques (Rakic et al. 1991; Dehay et al. 1996), rats (Sugita and Otani 1984; Laing et al. 2012), ferrets (Reillo et al. 2011), short-tailed opossum (Karlen and Krubitzer 2009), cat (Olavarria and Van Sluyters 1995), as well as MRI-based measurements in blind human subjects of the area size of V1 (Park et al. 2009), or of a pericalcarine area around V1 (Jiang et al. 2009). A piece-wise regression was performed on all data, with each data point weighted by the square-root of the sample size used to estimate that data point. In agreement with our present results, this analysis suggests the existence of a graded dependence of the surface area of V1 on the age of blindness onset that is consistent across species, yielding an $ET_c = 0.75$ (Fig. 7, black symbols).

In a similar manner, extant data on the development of the area size of V1 in sighted individuals can also be directly compared with the present findings. Such data include studies in rats (Duffy et al. 1998), cats (Duffy et al. 1998; Rathjen et al. 2003), macaques (Rakic et al. 1991; Purves and LaMantia 1993; Dehay et al. 1991, 1996; Horton and Hocking 1998), and humans (Lyall et al. 2015). These data on surface area maturation in normal development yields an estimated value of $ET_{dev} = 0.91$ (Fig. 7 blue symbols), well after the estimated value of $ET_c = 0.75$ obtained for effect of visual deprivation on surface area of V1. Thus, the analysis of published data on the development of the area size of V1 from a variety of mammalian species supports our observation that the effect of visual deprivation ceases its effect on V1 surface area expansion prior to the normal completion of V1 surface area expansion. Additionally, $ET_c$ also precedes the peak synaptic density in V1, which occurs at ET = 0.86, corresponding to postnatal day 23 in rats, postnatal day 58 in ferrets, and postnatal day 332 in humans (Workman et al. 2013).
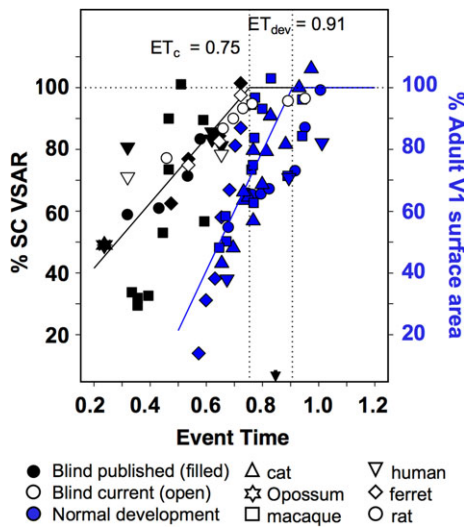
**Figure 7.** Inter-species comparison using a common developmental event-time scale (Workman et al. 2013) of the effect of age of blindness onset on the area size of V1 and the development of V1 area size in normal, sighted individuals. Our current data on the effect of blindness (open symbols), presented in Fig. 4, are plotted together with data from published studies on the effect of blindness on the size of V1 in different species (black symbols). Our data for the development of the area size of V1 in normal, sighted rats presented in Fig. 6 are plotted together with data from published studies on the development of V1 area size in different species (blue symbols, and blue Y-axis legend). The black and blue segmented regression lines were weighted by the sample size (either one or several cases) for each data point. Dashed horizontal line corresponds to 100% of sighted control VSAR, while dotted vertical lines indicate the intersection points marking the event times for the estimated $ET_c = 0.75$ (adj. $R^2 = 0.53$), and $ET_{dev} = 0.91$ (adj. $R^2 = 0.56$). These event times indicate the end of the critical period for the effect of enucleation on the area size of V1, and the event time at which area V1 reaches its normal adult size in sighted individuals, respectively. This inter-species comparison confirms our observation that blindness ceases to affect the surface area of area V1 before expansion of V1 is complete, and extends it to many mammalian species. Extant data on the effect of visual deprivation on the size of V1 come from histological studies in rhesus macaques (Rakic et al. 1991; Dehay et al. 1996), rats (Sugita and Otani 1984; Laing et al. 2012), ferrets (Reillo et al. 2011), short-tailed opossum (Karlen and Krubitzer 2009), cat (Olavarria and Van Sluyters 1995), as well as MRI-based studies of blind human subjects (Jiang et al. 2009; Park et al. 2009). Extant data on the development of the area size of V1 in sighted individuals include studies in rats (Duffy et al. 1998), cats (Duffy et al. 1998; Rathjen et al. 2003), macaques (Rakic et al. 1991; Purves and LaMantia 1993; Dehay et al. 1991, 1996; Horton and Hocking 1998), human (Lyall et al. 2015).

## Discussion

A wide variety of studies in both animals and humans have reported that early blindness results in reduced V1 surface area. However, the conclusion of the critical period for this effect, and its relationship to cortical expansion, has not previously been systematically compared among species. Here, we show that the conclusion of the period of susceptibility to blindness as a function of age of deprivation is remarkably consistent across species once data have been represented in a common developmental event-time framework (Workman et al. 2013). This critical period spans early to mid-cortical expansion, and ends before cortical expansion is complete, and well before cortical pruning begins. The increase in visual cortical thickness secondary to blindness reported by Bridge et al. (2009), as well as by other studies (Jiang et al. 2009; Park et al. 2009; Anurova et al. 2015), is thought to reflect a reduction in synaptic pruning. In this context, our results raise the possibility that V1 cortical thickness is regulated by biological processes

different from those governing V1 surface area. Analyzing the developmental trajectory of changes in cortical thickness caused by visual deprivation may help address this issue. In macaque monkeys, the effects of enucleation on the area size of V1 have been linked to the partial re-specification of striate cortex into hybrid cortex, named area X (Rakic 1988; Rakic et al. 1991), but this mechanism does not appear to be general across species. For instance, studies in anophthalmic (Bravo and Inzunza 1994) and enucleated rats (Laing et al. 2012), and enucleated ferrets (Bock et al. 2012) report a reduction of the area size of V1 without a re-specification of striate cortex, nor enlargement of extrastriate areas. The effects of enucleation on the size of visual cortex have also been linked to disruption of normal, prenatal thalamic influences on cortex development (Rakic 1988; Dehay et al. 2001; Dehay and Kennedy 2007; Reillo et al. 2011; Moreno-Juan et al. 2017).

Analysis of the results presented here indicate that enucleations performed at or after postnatal day P22 (ET = 0.86) in the rat, and P33 (ET = 0.74) in the ferret cease to affect the surface area expansion of V1. In humans, reductions in surface area were observed for both AN (ET = 0.32) and in the right hemisphere of EB (ET = 0.62) groups as compared with SC, and these reductions were similar in magnitude to those found in animal models. However, the VSAR in the LB group did not differ significantly from the SC group. Since blindness in the LB group occurred at ages corresponding to ET far greater than one, we could not determine with accuracy the end of the critical period for V1 surface area reductions in humans. A meta-analysis in which we combined our data from rats, ferrets and humans with animal and human data from previous studies, indicates that the end of the critical period for the effect of blindness on the area size of V1 is reached at $ET_C = 0.75$. In humans, this suggests that blindness would be expected to influence the surface area of V1 only if the onset occurs before P116. Given that, in visually normal individuals visual acuity is correlated with cortical surface area (Duncan and Boynton 2003), this result has interesting translational implications in cases of sight recovery. For example, a study examining individuals who suffered from congenital cataracts until the ages of 8–17 years of age found severe acuity losses, even many months after surgery (Kalia et al. 2014). It is possible that losses in V1 surface area are related to these impairments in pattern vision.

Although this study was not designed to determine the age at which retinal input begins to influence the expansion of visual cortex, available information suggests that this occurs before P4 (ET = 0.53) in the rat (Laing et al. 2012), and P7 (ET = 0.54) in the ferret (Reillo et al. 2011; Bock et al. 2012). In macaques, Rakic et al. (1991) and Dehay et al. (1996) reported that the effects of BEP on the size of V1 remains about the same for enucleations performed at ET = 0.334, 0.355, and 0.393 (Fig. 7, black squares). In contrast, the reduction in the size of V1 was significantly smaller for enucleation performed at ET = 0.445 (Dehay et al. 1996), suggesting that retinal input starts influencing the size of V1 sometime between ET = 0.393 (PC 68) and ET = 0.445 (PC 77). Retinal axons reach the LGN by ET = 0.319, and axons from the LGN synapse onto subplate neurons of the developing primary visual cortex between ET 0.3 and 0.53 (Workman et al. 2013). Thus, consistent with previous studies of the role of thalamic afferents during cortical development (Rakic 1988; Dehay et al. 2001; Dehay and Kennedy 2007; Reillo et al. 2011; Moreno-Juan et al. 2017), the age at which retinal input starts influencing the area size of V1 in macaques, and perhaps other species, may correlate with the arrival of thalamic axons in visual cortex, and formation of synapses.

## The Effect of Blindness on Surface Area Ends Before Cortical Expansion is Complete

The period during which the surface area of V1 is susceptible to blindness is relatively protracted compared with other critical periods in cortical development. For example, the critical period for the effect of visual input on corticocortical connection patterns in rats is confined to an approximately 2-day time interval from P4 to P6 (ET = 0.53–0.58) (Olavarria et al. 1987; Olavarria and Hiroi 2003; Laing et al. 2012). Similarly, in ferrets, the period in which the pattern of visual callosal connections is susceptible to enucleation ends during the third postnatal week (ET = 0.65) (Bock et al. 2012). In contrast, our estimate of the end of the critical period for surface area is $ET_c$ = 0. 74, suggesting that visual input continues to regulate the size of visual cortex well after the corticocortical connections of visual cortex have been specified. Cortical expansion occurs relatively late in the neuro-developmental timeline compared with the establishment of corticocortical connections. For example, while corticocortical connections in rats appear mature by P12 (ET = 0.69) (Olavarria and Van Sluyters 1985), the area of V1 reaches its adult size more than two weeks later. In rats, we found that V1 reaches its adult size by P40 (ET = 1.05). This result is in good agreement with data for the growth of V1 in the cat (Duffy et al. 1998) showing that by 12 weeks of age (ET = 0.97) the areal extent of V1 is adult-like. Thus, visual input regulates multiple aspects of cortical development through mechanisms that operate during different time windows. Similarly, in ferrets, the critical period for the effect of enucleation on the area size of V1 ends by P33 (ET = 0.74), but normal cortical expansion continues at least until P59 (ET = 0.87, unpublished findings). In humans, cortical expansion is even more prolonged; cerebral cortex reaches ~95% of its adult volume by 6 years of age (Giedd et al. 2015). Our present analysis suggests that the critical period for visual deprivation ends by $ET_c$ = 0. 75, corresponding to approximately postnatal Week 17 in humans. Thus, visual cortical expansion seems to consist of an initial stage that is susceptible to visual deprivation, and a later stage during which expansion is largely independent of ongoing visual input. Our meta-analysis including data from previous studies in other species suggests that these results can be generalized to many mammalian species.

One potential consequence of cortical expansion occurring relatively late in the developmental timeline is that it may allow the specification of V1 intra-cortical connections to match the statistics of visual input. Some aspects of visual development are surprisingly slow to reach a mature state. For example, human foveal development, reflected by cone packing density and foveal diameter does not reach adult measures until sometime after 45 months postnatal (Yuodelis and Hendrickson 1986). In visually normal individuals there is a 2- to 3-fold variation in the size of the optic tract, the volumes of the magnocellular and parvocellular layers of the LGN, and the surface area and volume of V1. Importantly, this variation is coordinated within the visual system of any one individual. That is, a relatively large V1 is associated with a commensurately large LGN and optic tract, whereas a relatively small V1 is associated with a commensurately smaller LGN and optic tract (Andrews et al. 1997). These variations seem to influence visual performance: visual acuity is correlated with cortical surface area (Duncan and Boynton 2003), both as a function of eccentricity, and across individuals. This relationship across the hierarchy of the human visual pathway suggests that the development of its different parts is interdependent (Andrews et al. 1997), and may explain why cortical expansion occurs relatively late in the neuro-developmental timeline.

## The Neuro-developmental Context for the Effects of Visual Deprivation on Surface Area

The use of a common developmental event-time framework permits the cross-species comparison of the conclusion of the critical period for the effect of visual deprivation on cortical surface area. Enucleation in rats and ferrets, or blindness onset in humans at ETs 0.25, 0.5, or 0.7 (see Fig. 7), are associated with primary visual cortical surface areas at maturity that are ~50%, 70%, or 90% of the surface area of primary visual cortex in normally-SC, respectively. At ET 0.25, retinal axons have begun to form the optic tract, but their terminals do not reach the lateral geniculate nucleus until an event time of 0.319 (Workman et al. 2013). Thalamic axons from the LGN influence mitogenic activity within subcortical lamina of the occipital lobe (Dehay et al. 2001; Dehay and Kennedy 2007; Reillo et al. 2011), and synapse onto subplate neurons of the developing primary visual cortex between ET 0.3 and 0.53 (post-conception age 28 to P6 in the ferret) (Johnson and Casagrande 1993; Herrmann et al. 1994). According to Reillo et al. (2011), a special type of progenitor cells leads to the generation of a class of glial cells that promote tangential dispersion of radially migrating neurons, and thereby facilitates growth in surface area of the cortical sheet. Disruption of the thalamic afferents through early enucleation in ferrets at P2 (ET = 0.49) reduces the density of these progenitor cells which in turn is associated with a reduction in cortical surface area (Reillo et al. 2011). Thus, the ~30% reduction in visual cortex surface area observed in early enucleated animals (Figs 1 and 2) and anophthalmic subjects (Fig. 3), who are deprived at the equivalent of ET 0.32 or earlier, is consistent with the idea that visual deprivation reduces cortical surface area by interfering with the effect of these progenitor cells on surface area expansion. At an ET of 0.5, retinal axons innervate the thalamus; thalamic axons have synapsed with subplate, but not layer IV neurons. Neurogenesis of cortical neurons is essentially complete, but intra-cortical synaptogenesis has yet to begin, and the eyes have not yet opened (Workman et al. 2013). Human EB individuals were deprived of retinal input beginning approximately in the second half of human gestation (ET = 0.62). At this ET myelination of the optic radiations is complete, and myelination of the optic tract is underway. Thus, the effects of spontaneous neural activity in the retina and LGN are likely to influence maturation of the cerebral cortex in the early blind group to an extent. It is possible that prenatal thalamic waves (Moreno-Juan et al. 2017) acting directly, or through the release of diffusible factors (Dehay et al. 2001; Dehay and Kennedy 2007), regulate the increase of cortical area size during development. Within cortex, synaptogenesis as well as differentiation of individual cortical layers is underway. It remains to be seen whether the effects seen in EB subjects and animals enucleated later in development simply reflect the asymptotic effects of cortical tangential expansion, or whether the smaller reduction in visual cortex size observed in these individuals also involves perturbation of the initial formation of visual cortical circuits.

## Human versus Animal Data

One limitation of studies examining the effects of visual deprivation on cortical anatomy in humans is that it is extremely difficult to systematically examine the effects of age of

deprivation in the human population. While it is possible to find relatively homogenous subject groups affected with anophthalmia or early blindness, it is essentially impossible to examine the effects of age within prenatal development, and extremely challenging to find a subject group where deprivation systematically spans early childhood development.

Another limitation of human studies is that visual deprivation results from a variety of pathologies that differ widely both in disease mechanism (e.g., photoreceptor disease vs. optic nerve damage) and in the extent of visual deprivation (no retinal signals vs. light perception). Thus, while blindness in the rats and ferrets in this study was induced by BEP, within our human populations, most individuals maintained at least some retinal projections. Indeed, five of the EB subjects and most of the LB subjects had low light perception (but no form perception) (Supplementary Table S1). It should also be noted that, due to the etiology of blindness, the timing of blindness onset could not be determined with precision in many EB and LB cases. Perhaps surprisingly, the presence of residual light perception did not seem to influence cortical surface area in EB individuals. No significant difference in cortical surface area was found across the EB individuals with and without light perception. Moreover, when projected onto a common developmental timeline, EB individuals showed similar magnitudes of reductions in surface area as observed in enucleated animals. This failure to find a difference between enucleation and light deprivation due to photoreceptor loss suggests that the mechanisms underlying later tangential expansion can be disrupted by loss of pattern vision, as well as by the absence of the retino-LGN-V1 projection.

Translating data from several species into a common developmental time scale revealed a striking similarity across species both in the size of the reduction of surface area, and in the relationship between the graded reduction in visual cortical surface area and the age of blindness onset. This allowed us to estimate that visual deprivation starting at $ET_c = 0.75$ no longer affects the surface area of V1. In humans, this event time corresponds to postnatal Day 116. We also found that the critical period for the effect of visual deprivation ends long before cortical expansion is complete. Efforts to confirm these ETs for humans will require finding subject groups whose blindness onset spans early childhood development, including the first year of life.

In conclusion, our findings suggest that visual deprivation disrupts mechanisms that influence early stages of cortical expansion. In humans, the critical period for the effect of visual deprivation on visual surface area ends near the first year of life, suggesting that the age of deprivation may play a significant role in anatomical specification up to that age. Thus, this critical period may have translational importance when considering the likely success of sight recovery procedures in individuals blinded before the first year of life. Visual deprivation during later stages of cortical expansion, or during cortical pruning had little or no effect on V1 surface area. No significant difference was found between EB individuals with light perception and those without, suggesting that, at postnatal stages, it is the absence of patterned vision that is important. Further work will be needed to understand the mechanisms by which loss of visual input disrupts V1 cortical expansion, and why their influence ceases before expansion of V1 is complete.

## Supplementary Material

Supplementary material is available at *Cerebral Cortex* online.

## Funding

## Notes

## References

Andrews TJ, Halpern SD, Purves D. 1997. Correlated size variations in human visual cortex, lateral geniculate nucleus, and optic tract. J Neurosci. 17:2859–2868.

Anurova I, Renier LA, DeVolder AG, Carlson S, Rauschecker JP. 2015. Relationship between cortical thickness and functional activation in the early blind. Cereb Cortex. 25: 2035–2048.

Benson NC, Butt OH, Ritobrao D, Radoeva PD, Brainard DH, Aguirre GK. 2012. The retinotopic organization of striate cortex is well predicted by surface topology. Curr Biol. 22: 2081–2085.

Bock AS, Binda P, Benson NC, Bridge H, Watkins KE, Fine I. 2015. Resting-state retinotopic organization in the absence of retinal input and visual experience. J Neurosci. 35: 12366–12382.

Bock AS, Kroenke CD, Taber EN, Olavarria JF. 2012. Retinal input influences the size and corticocortical connectivity of visual cortex during postnatal development in the ferret. J Comp Neurol. 520:914–932.

Bock AS, Olavarria JF, Leigland LA, Taber EN, Jespersen SN, Kroenke CD. 2010. Diffusion tensor imaging detects early cerebral cortex abnormalities in neuronal architecture induced by bilateral neonatal enucleation: an experimental model in the ferret. Front Sys Neurosci. 4:149.

Bourgeois JP, Rakic P. 1993. Changes in the synaptic density in the primate visual cortex of the macaque monkey from fetal to adult stage. J Neurosci. 13:2801–2820.

Bravo H, Inzunza O. 1994. Effect of pre- and postnatal retinal deprivation on the striate-peristriate cortical connections in the rat. Biol Res. 27:73–77.

Bridge H, Cowey A, Ragge N, Watkins K. 2009. Imaging studies in congenital anophthalmia reveal preservation of brain architecture in 'visual' cortex. Brain. 132:3467–3480.

Clancy B, Kersh B, Hyde J, Darlington RB, Anand KFS, Finlay BL. 2007. Web-based method for translating neurodevelopment from laboratory species to humans. Neuroinformatics. 5: 79–94.

Dale AM, Fischl B, Sereno MI. 1999. Cortical surface-based analysis. I. Segmentation and surface reconstruction. Neuroimage. 9:179–194.

Darlington RB, Dunlop SA, Finlay BL. 1999. Neural development in metatherian and eutherian mammals: variation and constraint. J Comp Neurol. 411:359–368.

Dehay C, Giroud P, Berland M, Killackey H, Kennedy H. 1996. Contribution of thalamic input to the specification of cytoarchitectonic cortical fields in the primate: effects of bilateral enucleation in the fetal monkey on the boundaries, dimensions, and gyrification of striate and extrastriate cortex. J Comp Neurol. 367:70–89.

Dehay C, Horsburgh G, Berland M, Killackey H, Kennedy H. 1989. Maturation and connectivity of the visual cortex in monkey is altered by prenatal removal of retinal input. Nature. 337:265–267.

Dehay C, Horsburgh G, Berland M, Killackey H, Kennedy H. 1991. The effects of bilateral enucleation in the primate fetus on the parcellation of visual cortex. Dev Brain Res. 62: 137–141.

Dehay C, Kennedy H. 2007. Cell-cycle control and cortical development. Nat Rev Neurosci. 8:438–450.

Dehay C, Savatier P, Cortay V, Kennedy H. 2001. Cell-cycle kinetics of neocortical precursors are influenced by embryonic thalamic axons. J Neurosci. 21:201–214.

Duffy KR, Murphy KM, Jones DG. 1998. Analysis of the postnatal growth of visual cortex. Vis Neurosci. 15:831–839.

Duncan RO, Boynton GM. 2003. Cortical magnification within human primary visual cortex correlates with acuity thresholds. Neuron. 38:659–671.

Finlay BL, Darlington RB. 1995. Linked regularities in the development and evolution of mammalian brains. Science. 268: 1578–1584.

Fischl B. 2004. Automatically parcellating the human cerebral cortex. Cereb Cortex. 14:11–22.

Fischl B, Rajendran N, Busa E, Augustinack J, Hinds O, Yeo BTT, Mohlberg H, Amunts K, Zilles K. 2008. Cortical folding patterns and predicting cytoarchitecture. Cereb Cortex. 18: 1973–1980.

Fischl B, Salat DH, Busa E, Albert M, Dieterich M, Haselgrove C, van der Kouwe A, Killiany R, Kennedy D, Klaveness S, et al. 2002. Whole brain segmentation: automated labeling of neuroanatomical structures in the human brain. Neuron. 33:341–355.

Giedd JN, Raznahan A, Alexander-Bloch A, Schmitt E, Gogtay N, Rapoport JL. 2015. Child psychiatry branch of the National Institute of Mental Health longitudinal structural magnetic resonance imaging study of human brain development. Neuropsychopharm Rev. 40:43–49.

Herrmann K, Antonini A, Shatz CJ. 1994. Ultrastructural evidence for synaptic interactions between thalamocortical axons and subplate neurons. Eur J Neurosci. 6:1729–1742.

Hinds O, Polimeni JR, Rajendran N, Balasambramanian M, Wald LL, Augustinack JC, Wiggins G, Rosas HD, Fischl B, Schwarz EL. 2008. The intrinsic shape of human and macaque primary visual cortex. Cereb Cortex. 18:2586–2595.

Horton JC, Hocking DR. 1998. Effect of early monocular enucleation upon ocular dominance columns and cytochrome oxidase activity in monkey and human visual cortex. Visual Neurosci. 15:289–303.

Huttenlocher PR. 1990. Morphometric study of human cerebral cortex development. Neuropsychol. 28:517–527.

Jiang F, Stecker GC, Boynton GM, Fine I. 2016. Early blindness results in developmental plasticity for auditory motion processing within auditory and occipital cortex. Front Hum Neurosci. 10:324.

Jiang J, Zhu W, Shi F, Liu Y, Li J, Qin W, Li K, Yu C, Jiang T. 2009. Thick visual cortex in the early blind. J Neurosci. 29:2205–2211.

Johnson JK, Casagrande VA. 1993. Prenatal development of axon outgrowth and connectivity in the ferret visual system. Vis Neurosci. 10:117–130.

Kalia A, Lesmes LA, Dorr M, Gandhi T, Chatterjee G, Ganesh S, Bex PJ, Sinha P. 2014. Development of pattern vision following early and extended blindness. Proc Natl Acad Sci USA. 111:2035–2039.

Karlen SJ, Krubitzer L. 2009. Effects of bilateral enucleation on the sizes of visual and nonvisual areas of the brain. Cereb Cortex. 19:1360–1371.

Knutsen AK, Kroenke CD, Chang YV, Taber LA, Bayly PV. 2013. Spatial and temporal variations of cortical growth during gyrogenesis in the developing ferret brain. Cereb Cortex. 23:488–498.

Konietschke F, Placzek M, Schaarschmidt F, Hothorn LA. 2015. nparcomp: An R software package for nonparametric multiple comparisons and simultaneous confidence intervals. J Stat Softw. 64:1–17.

Laing RJ, Bock AS, Lasiene J, Olavarria JF. 2012. Role of retinal input on the development of striate-extrastriate patterns of connections in the rat. J Comp Neurol. 520:3256–3276.

Laing RJ, Lasiene J, Olavarria JF. 2013. Topography of striate-extrastriate connections in neonatally enucleated rats. Biomed Res Int. 2013:592426.

Laing RJ, Turecek J, Takahata T, Olavarria JF. 2015. Identification of eye-specific domains and their relation to callosal connections in primary visual cortex of Long Evans rats. Cereb Cortex. 25:3314–3329.

Lepore N, Voss P, Lepore F, Chou Y-Y, Fortin M, Gougoux F, Lee AD, Brun C, Lassonde M, Madsen SK, et al. 2010. Brain structure changes visualized in early-and late-onset blind subjects. Neuroimage. 49:134–140.

Lyall AE, Shi F, Geng X, Woolson S, Li G, Wang L, Hamer RM, Shen D, Gilmore JH. 2015. Dynamic development of regional cortical thickness and surface area in early childhood. Cereb Cortex. 25:2204–2212.

Massé IO, Guillemette S, Laramée M-E, Bronchti G, Boire D. 2014. Strain differences of the effect of enucleation and anophthalmia on the size and growth of sensory cortices in mice. Brain Res. 1588:113–126.

Missler M, Eins S, Merker H-J, Rothe H, Wolff JR. 1993. Pre- and postnatal development of the primary visual cortex of the common marmoset. I. A changing space for synaptogenesis. J Comp Neurol. 333:41–52.

Moreno-Juan V, Filipchuk A, Antón-Bolaños N, Mezzera C, Gezelius H, Andrés B, Rodríguez-Malmierca L, Susín R, Schaad O, Iwasato T, et al. 2017. Prenatal thalamic waves regulate cortical area size prior to sensory processing. Nat Commun. 8:14172.

Olavarria JF, Bock AS, Leigland LA, Kroenke CD. 2012. Deafferentation-induced plasticity of visual callosal connections: predicting critical periods and analyzing cortical abnormalities using diffusion tensor imaging. Neural Plast. 2012:250196.

Olavarria JF, Hiroi R. 2003. Retinal influences specify corticocortical maps by postnatal day six in rats and mice. J Comp Neurol. 459:156–172.

Olavarria JF, Malach R, VanSluyters RC. 1987. Development of visual callosal connections in neonatally enucleated rats. J Comp Neurol. 260:321–348.

Olavarria J, Van Sluyters RC. 1985. Organization and post-natal development of callosal connections in the visual cortex of the rat. J Comp Neurol. 239:1–26.

Olavarria J, Van Sluyters RC. 1995. Overall pattern of callosal connections in visual cortex of normal and enucleated cats. J Comp Neurol. 363:161–176.

Park H-J, Lee JD, Kim EY, Park B, Oh M-K, Lee SC, Kim J-J. 2009. Morphological alterations in the congenital blind based on

the analysis of cortical thickness and surface area. Neuroimage. 47:98–106.

Ptito M, Schneider FCG, Paulson OB, Kupers R. 2008. Alterations of the visual pathways in congenital blindness. Exp Brain Res. 187:41–49.

Purves D, LaMantia A. 1993. Development of blobs in the visual cortex of macaques. J Comp Neurol. 334:169–175.

Rakic P. 1988. Specification of cerebral cortical areas. Science. 241:170–176.

Rakic P, Suner I, Williams RW. 1991. A novel cytoarchitectonic area induced experimentally within the primate visual cortex. Proc Nat Acad Sci USA. 88:2083–2087.

Rathjen S, Schmidt KE, Löwel S. 2003. Postnatal growth and column spacing in cat primary visual cortex. Exp Brain Res. 149:151–158.

Rauschecker JP, Tian B, Korte M, Egert U. 1992. Crossmodal changes in the somatosensory vibrissa/barrel system of visually deprived animals. Proc Nat Acad Sci USA. 89: 5063–5067.

Raznahan A, Shaw P, Lalonde F, Stockman M, Wallace GL, Greenstein D, Clasen L, Gogtay N, Giedd JN. 2011. How does your cortex grow? J Neurosci. 31:7174–7177.

Reillo I, Romero CDJ, Garcia-Cabezas MA, Borrell V. 2011. A role for intermediate radial glia in the tangential expansion of the mammalian cerebral cortex. Cereb Cortex. 21:1674–1694.

Richter CP, Warner CL. 1974. Comparison of Weigert stained sections with unfixed, unstained sections for study of myelin sheaths. Proc Nat Acad Sci USA. 71:598–601.

Stevens AA, Snodgrass M, Schwartz D, Weaver K. 2007. Preparatory activity in occipital cortex in early blind humans predicts auditory perceptual performance. J Neurosci. 40:10734–10741.

Sugita S, Otani K. 1984. Quantitative analysis of the striate cortex in the mutant microphthalmic rat. Exp Neurol. 85:584–596.

Trampel R, Ott DV, Turner R. 2011. Do the congenitally blind have a stria of gennari? First intracortical insights in vivo. Cereb Cortex. 21:2075–2081.

Verma AS, Fitzpatrick DR. 2007. Anophthalmia and microphthalmia. Orphanet J Rare Dis. 2:47.

Workman AD, Charvet CJ, Clancy B, Darlington RB, Finlay BL. 2013. Modeling transformations of neurodevelopmental sequences across mammalian species. J Neurosci. 33:7368–7383.

Yuodelis C, Hendrickson A. 1986. A qualitative and quantitative analysis of the human fovea during development. Vis Res. 26:847–855.